

Notes and Correspondence

An analytic solution for time-periodic thermally driven slope flows

D. Zardi^{a,b*} and S. Serafin^c

^aAtmospheric Physics Group, Department of Civil, Environmental and Mechanical Engineering, University of Trento, Italy

^bNational Consortium of Universities for Atmospheric and Hydrospheric Physics (CINFAI), Tolentino, Italy

^cDepartment of Meteorology and Geophysics, University of Vienna, Austria

*Correspondence to: D. Zardi, Atmospheric Physics Group, Department of Civil, Environmental and Mechanical Engineering, University of Trento, Via Mesiano 77, I-38123 Trento, Italy. E-mail: Dino.Zardi@unitn.it

The article examines the flow generated by time-periodic variations in surface temperature along an infinite slope in an initially unperturbed, stably stratified atmosphere at rest. Uniform boundary conditions at the surface are conducive to an along-slope parallel flow, governed by a periodically reversing local imbalance between along-slope advection and slope-normal fluxes of momentum and heat. It is shown that solutions include both a transient part and a periodic regime and that three different flow regimes may occur. The properties of the solutions in each regime are examined and discussed, outlining novelties with respect to previously known results.

Key Words: thermally driven wind; topographic effects; slope flows; Prandtl model

Received 17 June 2014; Revised 13 October 2014; Accepted 20 October 2014; Published online in Wiley Online Library

1. Introduction

The flow generated over a *simple slope* (i.e. an infinitely extended tilted plane) by surface heating or cooling provides a basic paradigm for understanding thermally driven mountain wind systems (Zardi and Whiteman, 2013).

One of the best known models of steady slope flow was proposed by Prandtl (1942). The model describes the steady flow resulting from a balance between along-slope advection and slope-normal fluxes of momentum and heat, in an otherwise motionless, stably stratified atmosphere. Despite their inherently restrictive assumptions, Prandtl's (1942) solutions reproduce realistic downslope flow reasonably well. This has been confirmed by both field measurements (Defant, 1949; Axelsen and van Dop, 2009a) and high-resolution numerical simulations (Skylingstad, 2003; Smith and Skylingstad, 2005; Axelsen and van Dop, 2009b). The agreement with upslope flows is less satisfactory, as both field measurements (Defant, 1949) and numerical simulations (Schumann, 1990; Serafin and Zardi, 2010b) demonstrate. Nevertheless, the Prandtl model provides a solid framework by which to understand the mechanisms involved in the production of thermally driven slope flows (cf. Fedorovich and Shapiro, 2009).

Prandtl's approach was further extended by various authors, who found analytical solutions capable of describing the effects of a number of secondary forcing factors. For instance, Grisogono and Oerlemans (2001) and Grisogono *et al.* (2014) applied a WKB technique to account for a non-constant eddy viscosity. Zammett and Fowler (2007) found an approximate solution representing the effects of a slowly changing slope angle, resulting in a varying along-slope velocity and a non-zero slope-normal velocity component. Stiperski *et al.* (2007) derived an analytical

solution including Coriolis effects. However, all of the above solutions refer to steady states.

A model allowing the slope flow system to evolve in time was proposed by Gutman and Malbakhov (1964). Their theory, which included both surface thermal forcing and the Coriolis effect, aimed at understanding the onset of katabatic winds and their adjustment to changes in the upper forcing. Vertical velocity profiles from the Gutman and Malbakhov (1964) model were reported to be in good agreement with soundings taken in Antarctica.

However, the first historical attempt at including time-dependent behaviour in slope-flow models was published only a few years after Prandtl's original work. Defant (1949) extended Prandtl's (1942) theory in order to allow for a time-periodic surface temperature forcing. As a result, Defant's model displays the slope-normal structure of Prandtl's one, modulated by the same time-periodic dependence of the surface forcing. Accordingly, it entails a periodic time-reversal of the flow and the temperature anomaly, occurring in phase at any height above the slope. However, a careful examination of Defant's (1949) expressions reveals that they are only an approximation of the exact time-dependent solutions, which are derived in section 2 below. The properties of the exact solutions in three cases of interest are outlined in section 3, while conclusions are drawn in section 4.

2. Formulation of the problem

The flow occurring along an infinitely extended plane, tilted by an angle α to the horizontal, is inherently one-dimensional. Following Prandtl (1942), it can conveniently be studied in a reference frame with an along-slope coordinate s (positive

upslope) and a slope-normal coordinate n (Figure 1). The coordinate axes are rotated counterclockwise by an angle α , with respect to a reference frame having the z -axis aligned with gravity and oriented upward and the x -axis along the horizontal.

Let potential temperature be represented as $\theta = \theta_r + \bar{\theta} + \theta'$, where $\theta_r = \theta_0 + \gamma z$ is the thermal structure of the unperturbed atmosphere, displaying a constant vertical gradient γ . $\bar{\theta}$ and θ' denote respectively the mean and fluctuating components—in the sense of Reynolds decomposition—of the turbulent perturbation determined by the thermal forcing at the surface. In analogy, the along-slope velocity component will be decomposed into $u = \bar{u} + u'$ and the slope-normal one into $w = \bar{w} + w'$.

Similarly to gravity waves in stratified fluids, slope flows can be studied more easily if the Boussinesq approximation is assumed; in the present case, the Coriolis force is neglected. In contrast to the linear theory of gravity waves, turbulent diffusion terms have to be retained here. We further assume invariance along the s -axis. As a consequence, incompressibility—following from the Boussinesq approximation—implies that slope-normal velocity perturbations \bar{w} associated with the slope flow system are null. Pressure perturbations are instead determined by quasi-hydrostatic balance along the n -axis (Haiden, 2003). Accordingly, the Reynolds-averaged momentum and energy equations for an s -invariant, slope-parallel flow can be written as

$$\frac{\partial \bar{u}}{\partial t} = \bar{\theta} \frac{N^2}{\gamma} \sin \alpha - \frac{\partial \overline{u'w'}}{\partial n}, \quad (1)$$

$$\frac{1}{\rho_0} \frac{\partial \bar{p}}{\partial n} = \bar{\theta} \frac{N^2}{\gamma} \cos \alpha - \frac{\partial \overline{w'^2}}{\partial n}, \quad (2)$$

$$\frac{\partial \bar{\theta}}{\partial t} = -\bar{u} \gamma \sin \alpha - \frac{\partial \overline{w'\theta'}}{\partial n}, \quad (3)$$

where $N = (\gamma g / \theta_0)^{1/2}$ is the Brunt–Väisälä frequency of the unperturbed atmosphere, \bar{p} is the Reynolds-averaged pressure anomaly with respect to the unperturbed state and ρ_0 is the reference air density of the unperturbed atmosphere. As shown below, the coupled partial differential equations (1) and (3) can be solved analytically, provided that suitable closures for the turbulent fluxes are assumed and appropriate boundary conditions are specified. Equation (2) can instead be used in order to diagnose pressure perturbations, once the solution for $\bar{\theta}$ is known.

A simple way to approximate turbulent fluxes is a first-order K closure:

$$\overline{u'w'} = -K_m \frac{\partial \bar{u}}{\partial n}, \quad \overline{w'\theta'} = -K_h \frac{\partial \bar{\theta}}{\partial n}. \quad (4)$$

As a further simplification, we assume constant eddy viscosity K_m and eddy heat diffusivity K_h , finally getting the following coupled equations for \bar{u} and $\bar{\theta}$:

$$\frac{\partial \bar{u}}{\partial t} = \bar{\theta} \frac{N^2}{\gamma} \sin \alpha + K_m \frac{\partial^2 \bar{u}}{\partial n^2}, \quad (5)$$

$$\frac{\partial \bar{\theta}}{\partial t} = -\bar{u} \gamma \sin \alpha + K_h \frac{\partial^2 \bar{\theta}}{\partial n^2}. \quad (6)$$

These equations were first derived by Defant (1949), as an extension of those proposed by Prandtl (1942) for a steady, laminar flow to a non-stationary, turbulent case.

They may also be viewed as a particular case (i.e. when Coriolis terms are neglected) of the more general set of equations considered by Gutman and Malbakhov (1964).

A first-order closure with constant eddy viscosity and diffusivity is a rather crude representation of turbulence. Nevertheless, it may allow considerable insight into the basic structure of turbulent flows, as shown by the previously mentioned studies by Gutman and Malbakhov (1964), Shapiro and Fedorovich (2004b,

2006), Stiperski *et al.* (2007), Zammatt and Fowler (2007) and Fedorovich and Shapiro (2009), which all adopted a similar approach.

Yet another remarkable example of use of a first-order closure with constant exchange coefficients is Ekman's (1905) model for the flow resulting from a balance between horizontal pressure gradient, Coriolis force and turbulent momentum flux in the atmospheric boundary layer. Indeed, the similarity between Ekman's and Prandtl's solutions is one example of a general analogy between homogeneous, rotating fluids and stratified, non-rotating fluids, as pointed out by Veronis (1967).

2.1. Stationary problem (Prandtl, 1942)

Let us omit temporal derivatives from Eqs (5) and (6) and assume steady boundary conditions at the slope surface, consisting of no-slip for velocity and a prescribed constant temperature anomaly Θ :

$$\bar{u}(n=0) = 0, \quad \bar{\theta}(n=0) = \Theta. \quad (7)$$

Let us also require that perturbations vanish asymptotically far from the surface:

$$\bar{u}(n \rightarrow \infty) = 0, \quad \bar{\theta}(n \rightarrow \infty) = 0. \quad (8)$$

Then, a steady-state solution is easily found:

$$\bar{u} = \Theta \frac{N}{\gamma} \text{Pr}_t^{-1/2} e^{-n/\ell} \sin(n/\ell), \quad (9)$$

$$\bar{\theta} = \Theta e^{-n/\ell} \cos(n/\ell), \quad (10)$$

where $\text{Pr}_t = K_m/K_h$ is the turbulent Prandtl number, the length scale ℓ is

$$\ell = \left(\frac{4K_m K_h}{N_\alpha^2} \right)^{1/4}, \quad (11)$$

and $N_\alpha = N \sin \alpha$. The above expressions correspond to the solution found by Prandtl (1942), shown in Figure 1, once kinematic viscosity and heat diffusivity are replaced by eddy viscosity and diffusivity, respectively. The solution is equally valid for both heating and cooling at the surface: a positive (resp. negative) temperature anomaly at the surface will produce upslope (resp. downslope) flow. Notice that the length scale ℓ becomes singular for a horizontal surface ($\alpha = 0$), reflecting the fact that no steady balance can be achieved between along-slope advection and turbulent fluxes in the absence of some tilt

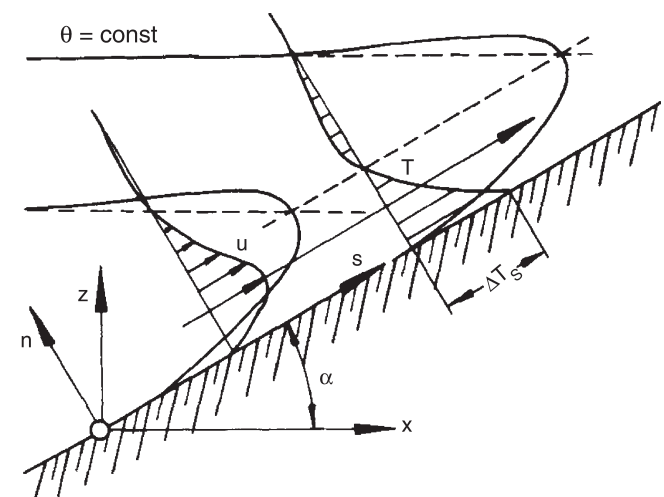


Figure 1. Prandtl (1942) solution (from Schumann, 1990, reproduced with permission). u , T and ΔT_s in the figure correspond respectively to \bar{u} , $\bar{\theta}$ and Θ in the text.

promoting an along-slope flow. Notice also that the length scale ℓ corresponds to Ekman's length scale, provided that K_h is replaced by K_m and N_α by the Coriolis parameter f .

Velocity and temperature perturbations in Prandtl's solution are $\pi/2$ out of phase along the slope-normal coordinate, exactly like velocity and temperature perturbations across phase lines in propagating gravity waves (Nappo, 2013).

Pressure perturbations can be diagnosed from Eqs (2) and (10) as

$$\bar{p} = \rho_0 \left\{ \frac{N^2}{2\gamma} \cos \alpha \Theta \ell e^{-n/\ell} [\sin(n/\ell) - \cos(n/\ell)] - \overline{w^2} \right\}. \quad (12)$$

Notice that the term $\overline{w^2}$ cannot be evaluated explicitly, unless a suitable closure is assumed for it. However a K closure cannot be easily applied in this case, since there is no mean velocity component in the slope-normal direction and accordingly no velocity gradient to compare with. Moreover, any attempt to relate the vertical velocity variance to the gradients of \bar{u} or $\bar{\theta}$, provided by Eqs (9) and (10), could not cope with the intrinsically positive nature of $\overline{w^2}$, as both gradients become negative at some point. Therefore, we leave this term undetermined.

However, concentrating on the resolved part of the pressure profile, it can be seen that pressure-velocity correlations are null on average. Therefore, differently from the case of gravity waves, perturbations in the slope flow system do not propagate in the slope-normal direction. Furthermore, they vanish with increasing distance from the slope because of turbulent, dissipative effects.

2.2. Non-stationary problem (Defant, 1949)

Following Defant (1949), let us now consider a stably stratified atmosphere initially at rest:

$$\bar{u}(n, 0) = 0, \quad \bar{\theta}(n, 0) = 0, \quad (13)$$

and assume zero velocity and a sinusoidally periodic temperature oscillation as surface boundary conditions:

$$\bar{u}(0, t) = 0, \quad \bar{\theta}(0, t) = \Theta \sin(\omega t + \psi). \quad (14)$$

Conditions far from the slope are the same as before.

Defant (1949) examined in particular the case $\psi = \pi/2$, i.e. $\bar{\theta}(0, t) = \Theta \cos(\omega t)$, and proposed a solution in the form

$$\bar{u} = \Theta \frac{N}{\gamma} \text{Pr}_t^{-1/2} e^{-n/\ell} \sin(n/\ell) \cos(\omega t), \quad (15)$$

$$\bar{\theta} = \Theta e^{-n/\ell} \cos(n/\ell) \cos(\omega t). \quad (16)$$

Equations (15) and (16) display the same spatial structure as the steady flow represented by Eqs (9) and (10), modulated in time by a factor $\cos(\omega t)$. Accordingly, they provide values of velocity and temperature anomaly oscillating in time with the same angular frequency ω as the surface forcing and in phase with it. At any height, the amplitude of oscillations is determined by the steady-state solution. Actually, Eqs (15) and (16) are not an exact solution of the system defined by the PDEs (Eqs (5) and (6)). They can, however, be shown to approximate a particular case of the general solution to the problem, as outlined below.

2.3. New solution

To make progress with the analytical solution, similarly to Gutman and Malbakhov (1964), Shapiro and Fedorovich (2004b), Zammett and Fowler (2007) and Stiperski *et al.* (2007), we need to impose $K_m = K_h = K$, i.e. $\text{Pr}_t = 1$. This assumption reflects the idea that molecular effects are relatively unimportant in this context and that heat and momentum are transported by turbulence with the same effectiveness (Lumley and Panofsky, 1964).

In the atmospheric surface layer over flat terrain, similarity theory suggests that $\text{Pr}_t = \phi_h/\phi_m$, where ϕ_m and ϕ_h are the similarity functions describing the non-dimensional vertical gradients of wind speed and temperature, respectively (Monin and Yaglom, 1971). In general, the exact value of ϕ_h/ϕ_m is a function of z/L , z being the distance from the ground and L the Obukhov length, and depends on the similarity functions of choice (ϕ_m and ϕ_h are not univocally determined: Sorbjan, 1989). It seems justified, however, to assume $\text{Pr}_t = 1$, at least in near-neutral conditions. The assumption $\text{Pr}_t = 1$ is also often adopted in numerical simulations of atmospheric boundary-layer flows (e.g. Khanna and Brasseur, 1997).

Under the condition $\text{Pr}_t = 1$, the length scale ℓ becomes

$$\ell = \left(\frac{2K}{N_\alpha} \right)^{1/2}. \quad (17)$$

Introducing the rescaled variable $\bar{v} = (\gamma\theta_0/g)^{1/2}\bar{u}$, Eqs (5) and (6) become

$$\frac{\partial \bar{v}}{\partial t} = N_\alpha \bar{\theta} + K \frac{\partial^2 \bar{v}}{\partial n^2}, \quad \frac{\partial \bar{\theta}}{\partial t} = -N_\alpha \bar{v} + K \frac{\partial^2 \bar{\theta}}{\partial n^2}. \quad (18)$$

Combining \bar{v} and $\bar{\theta}$ into the complex variable

$$\phi = \exp(-iN_\alpha t) (\bar{\theta} + i\bar{v}) \quad (19)$$

and rearranging Eq. (18), the problem is easily reduced to an initial-/boundary-value problem for the heat conduction equation for ϕ :

$$\frac{\partial \phi}{\partial t} = K \frac{\partial^2 \phi}{\partial n^2}, \quad (20)$$

with null initial condition and time-periodic boundary conditions at the surface, i.e.

$$\phi(n, 0) = 0, \quad \phi(0, t) = \exp(-iN_\alpha t) \Theta \sin(\omega t + \psi). \quad (21)$$

Solutions of the above problem are available in the literature (cf. Carslaw and Jaeger, 1959, p 64ff). Introducing the following parameters:

$$\omega_+ = N_\alpha + \omega, \quad \omega_- = N_\alpha - \omega, \quad (22)$$

$$\ell_+ = \left(\frac{2K}{\omega_+} \right)^{1/2}, \quad \ell_- = \left(\frac{2K}{\omega_-} \right)^{1/2}, \quad (23)$$

and defining

$$\eta = \frac{n}{2\sqrt{Kt}}, \quad (24)$$

the solution is

$$\begin{aligned} \phi(n, t) = & \frac{i\Theta}{\sqrt{\pi}} \int_0^\eta \left\{ \exp -i \left[\omega_+ t \left(1 - \frac{\eta^2}{\mu^2} \right) - \psi \right] \right. \\ & \left. - \exp -i \left[\omega_- t \left(1 - \frac{\eta^2}{\mu^2} \right) + \psi \right] \right\} e^{-\mu^2} d\mu \\ & + \frac{i\Theta}{2} \left\{ \exp \left[-i(\omega_+ t + \psi) - (1-i) \frac{n}{\ell_+} \right] \right. \\ & \left. - \exp \left[-i(\omega_- t - \psi) - (1-i) \frac{n}{\ell_-} \right] \right\}. \quad (25) \end{aligned}$$

Except for the special case $N_\alpha = \omega$ (see below), the integral term decays in time as $t \rightarrow \infty$ (cf. Carslaw and Jaeger, 1959, section 2.6, p. 65) and represents a transient disturbance caused

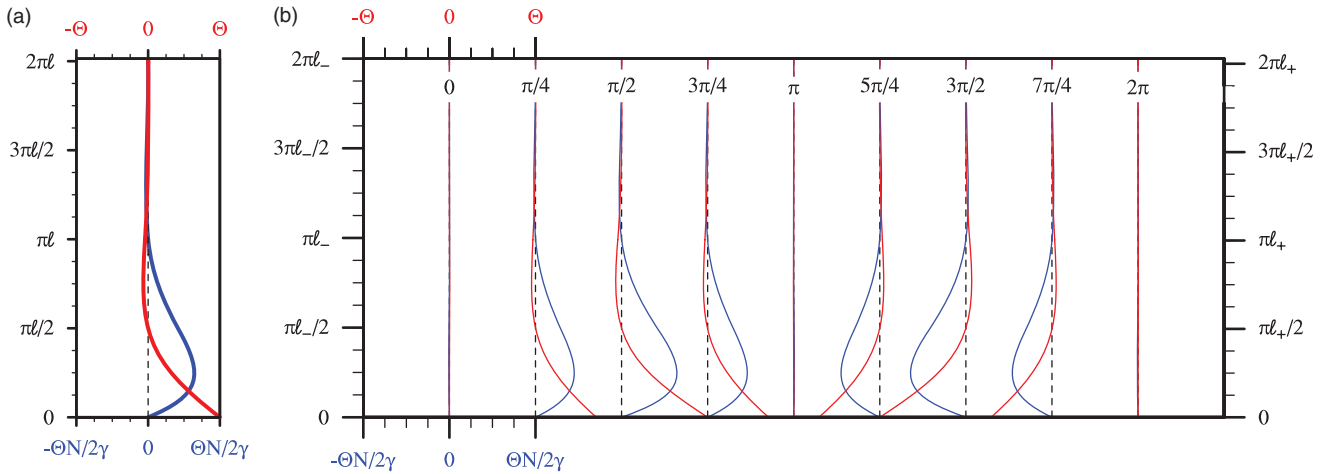


Figure 2. Slope-normal profiles of along-slope velocity \bar{u} (dark grey lines; blue in online) and potential temperature anomaly with respect to the unperturbed situation $\bar{\theta}$ (light grey lines; red in online) under supercritical conditions ($N_\alpha > \omega$). (a) Steady-state Prandtl (1942) solution for constant surface potential temperature anomaly Θ . (b) Vertical profiles at different values of ωt , as indicated at the top of each profile. Numerical values: $\alpha = 30^\circ$, $\Theta = 5 \text{ K}$, $\theta_0 = 288 \text{ K}$, $\gamma = 0.003 \text{ K m}^{-1}$, $\omega = 7.28 \times 10^{-5} \text{ s}^{-1}$, $K = 3 \text{ m}^2 \text{ s}^{-1}$, $\psi = 0$.

by starting the oscillations of surface temperature at time $t = 0$. The second term is the time-periodic component of the solution.

Equation (25) is somewhat analogous to the time-dependent model proposed by Shapiro and Fedorovich (2010) to describe nocturnal low-level jets, i.e. inertial oscillations of the wind speed and direction caused by the release of the frictional constraint in the Ekman boundary layer at sunset. Not surprisingly, the general analogy between the stationary Prandtl and Ekman solutions, mentioned in section 2 above, is also manifested in their time-dependent counterparts.

Reverting to the original variables, one finally obtains

$$\begin{aligned} \bar{\theta} + i\frac{\gamma}{N}\bar{u} = & \frac{i\Theta}{\sqrt{\pi}} \int_0^\eta \left\{ \exp i \left[\left(\omega + \omega_- \frac{\eta^2}{\mu^2} \right) t + \psi \right] \right. \\ & \left. - \exp i \left[\left(-\omega + \omega_+ \frac{\eta^2}{\mu^2} \right) t + \psi \right] \right\} e^{-\mu^2} d\mu \\ & + \frac{i\Theta}{2} \left\{ \exp \left[-i \left(\omega t - \frac{n}{\ell_+} + \psi \right) - \frac{n}{\ell_+} \right] \right. \\ & \left. - \exp \left[i \left(\omega t + \frac{n}{\ell_-} + \psi \right) - \frac{n}{\ell_-} \right] \right\}. \end{aligned} \quad (26)$$

3. Discussion of the solutions

Here we concentrate on the properties of the periodic part of the solution, which may assume three different forms, depending on the frequencies ω and N_α .

3.1. Case 1. Supercritical: $N_\alpha > \omega$

This case occurs for strong stability and/or large slope angle α . We refer to it as *supercritical*, because the time scale of the periodicity in surface temperature is longer than the period of a buoyancy oscillation. Both ω_+ and ω_- are positive and, accordingly, ℓ_+ and ℓ_- are real and positive as well. The periodic part of the solution to the problem is obtained by neglecting the integral terms in Eq. (26), which describe a transient initial disturbance. It reads

$$\begin{aligned} \bar{u} = & \frac{\Theta N}{2\gamma} \left[e^{-n/\ell_+} \cos \left(\omega t - \frac{n}{\ell_+} + \psi \right) \right. \\ & \left. - e^{-n/\ell_-} \cos \left(\omega t + \frac{n}{\ell_-} + \psi \right) \right], \end{aligned} \quad (27)$$

$$\begin{aligned} \bar{\theta} = & \frac{\Theta}{2} \left[e^{-n/\ell_+} \sin \left(\omega t - \frac{n}{\ell_+} + \psi \right) \right. \\ & \left. + e^{-n/\ell_-} \sin \left(\omega t + \frac{n}{\ell_-} + \psi \right) \right]. \end{aligned} \quad (28)$$

An example of the solution for the supercritical case is shown in Figure 2, where $\psi = 0$ is assumed. It may be noticed that this case displays a similar behaviour to Defant's model (Eqs (15) and (16)), apart from the different initial phase (0 instead of $\pi/2$). Indeed, at all heights both velocity and temperature oscillate approximately in phase, i.e. with no appreciable delay between near-surface and elevated layers. The zeros of both profiles remain essentially stationary over time.

It can be shown that Defant's model corresponds to a special case of Eqs (27) and (28), namely the condition $0 < \omega \ll N_\alpha$. In this case, $\omega_+ \approx \omega_- \approx N_\alpha$ and $\ell_+ \approx \ell_- \approx \ell$. Trigonometric addition formulae then immediately lead to Eqs (15) and (16), under the assumption $\text{Pr}_t = 1$. Therefore, Defant's (1949) model provides an acceptable description of time-dependent slope flows only when the time scale of variations in surface forcing is much longer than that of buoyancy oscillations in the atmosphere. Given typical values of atmospheric stratification and duration of the diurnal cycle, this condition is often verified. There is, however, a notable exception, namely the case of winds developing over gentle slopes in a near-neutral atmosphere ($N, \alpha \rightarrow 0$).

3.2. Case 2. Subcritical: $N_\alpha < \omega$

This case occurs for weak stability and/or small slope angles. Now ω_+ is positive and ω_- is negative. Accordingly, ℓ_+ is real and positive, whereas ℓ_- is an imaginary number. The time-periodic component of the solution in this case reads

$$\begin{aligned} \bar{u} = & \frac{\Theta N}{2\gamma} \left[e^{-n/\ell_+} \cos \left(\omega t - \frac{n}{\ell_+} + \psi \right) \right. \\ & \left. - e^{-n/|\ell_-|} \cos \left(\omega t - \frac{n}{|\ell_-|} + \psi \right) \right], \end{aligned} \quad (29)$$

$$\begin{aligned} \bar{\theta} = & \frac{\Theta}{2} \left[e^{-n/\ell_+} \sin \left(\omega t - \frac{n}{\ell_+} + \psi \right) \right. \\ & \left. + e^{-n/|\ell_-|} \sin \left(\omega t - \frac{n}{|\ell_-|} + \psi \right) \right]. \end{aligned} \quad (30)$$

An example of the solution for the subcritical case for $\psi = 0$ is shown in Figure 3. Notice that elevated layers may display a significant phase lag with respect to the layers adjacent to the surface. Consequently, upslope flow during a surface cooling phase (e.g. at $\omega t = 5\pi/4$) or, conversely, downslope flow during a surface warming phase (e.g. at $\omega t = \pi/4$) may occur. In contrast to the supercritical case, the zeros of both profiles move continuously away from the slope.

Subcritical solutions help us understand how the slope flow system behaves as the slope angle approaches zero or the

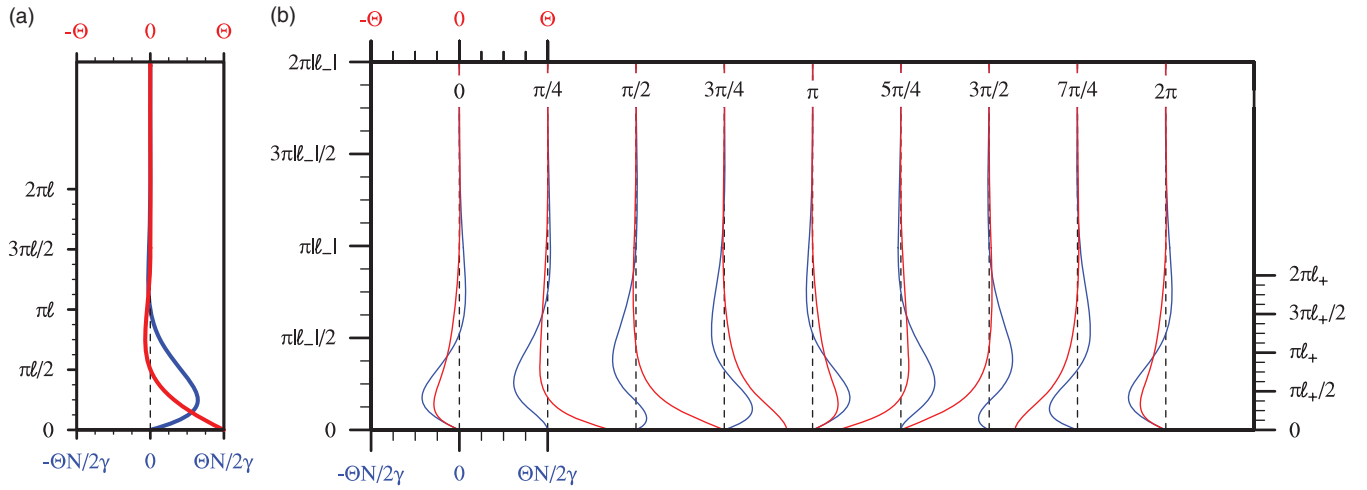


Figure 3. Same as in Figure 2, for a subcritical condition ($N_\alpha < \omega$). Numerical values: $\alpha = 0.5^\circ$, $\gamma = 0.001 \text{ K m}^{-1}$, $\psi = 0$.

atmosphere becomes neutrally stratified. For decreasing angles and/or stratification approaching neutrality, $\omega \gg N_\alpha \rightarrow 0$ and consequently $\ell_+ \rightarrow |\ell_-|$. In these conditions, in Eq. (29) the two terms in brackets tend to be identical in magnitude, so their difference vanishes. Therefore the wind speed tends to zero at all heights. On the other hand, Eq. (30) suggests that the potential temperature perturbation maintains a maximum at the surface. In other words, advection parallel to the surface ceases and heat is transported in the atmosphere solely by turbulent diffusion.

If, beyond $\alpha = 0$, a condition with invariant surface forcing is assumed ($\omega = 0$), Eq. (30) also collapses to 0. In this case, temperature perturbations are entirely determined by the non-periodic component of the full solution, i.e. by the integral term in Eq. (26). Actually, the solution is easily computed in this special case, resulting in

$$\bar{\theta} = \Theta \sin \psi \operatorname{erfc} \left\{ \frac{n}{2\sqrt{Kt}} \right\}; \quad (31)$$

that is, the potential temperature perturbation decreases with height but propagates to greater heights with increasing time. This well-known solution corresponds to heat diffusion after an impulsively started surface forcing.

3.3. Case 3. Critical: $N_\alpha = \omega$

In the critical case, the frequency of the forcing to the slope flow system matches the intrinsic frequency of buoyancy oscillations in the atmosphere. Consequently,

$$\omega_+ = 2\omega = 2N_\alpha, \quad \omega_- = 0, \quad (32)$$

$$\ell_+ = \left(\frac{K}{\omega} \right)^{1/2} = \left(\frac{K}{N_\alpha} \right)^{1/2}, \quad \ell_- = \infty. \quad (33)$$

In this circumstance, the full solution reads

$$\bar{u} = \frac{\Theta N}{2\gamma} \left\{ e^{-n/\ell_+} \cos \left(\omega t - \frac{n}{\ell_+} + \psi \right) - \operatorname{erfc}(\eta) \cos(\omega t + \psi) - \frac{2}{\sqrt{\pi}} \int_0^n \cos \left[\omega t \left(1 - \frac{2\eta^2}{\mu^2} \right) + \psi \right] e^{-\mu^2} d\mu \right\}, \quad (34)$$

$$\bar{\theta} = \frac{\Theta}{2} \left\{ e^{-n/\ell_+} \sin \left(\omega t - \frac{n}{\ell_+} + \psi \right) + \operatorname{erfc}(\eta) \sin(\omega t + \psi) - \frac{2}{\sqrt{\pi}} \int_0^n \sin \left[\omega t \left(1 - \frac{2\eta^2}{\mu^2} \right) + \psi \right] e^{-\mu^2} d\mu \right\}. \quad (35)$$

Critical solutions for both \bar{u} and $\bar{\theta}$ contain three terms in braces, the last of which vanishes as $t \rightarrow \infty$. The first term is

periodic in time, but it does not satisfy the boundary conditions for $n \rightarrow \infty$. The second one describes oscillations for which the amplitude, modulated by the factor $\operatorname{erfc}(\eta)$, decreases with height and increases in time. When taken together, these two terms do satisfy the upper boundary conditions; however, they do not describe a purely periodic behaviour any more.

An example of the solution for the critical case for $\psi = 0$ is shown in Figure 4, where the two leftmost terms of expressions (34) and (35), i.e. those that do not vanish in time, are considered. While the temperature profile still displays quasi-periodic oscillations, the depth of the atmospheric layer subject to motion increases steadily in time. The critical condition, where resonance occurs, seems to favour an efficient conversion of the surface energy fluxes into kinetic energy.

The special critical condition $\omega = N_\alpha = 0$ has been discussed in section 3.2 above, as a limiting case of subcritical behaviour.

4. Conclusions

A simple model describing the development of slope flows over an infinitely long and uniformly heated (or cooled) slope, the temperature of which varies periodically in time, is presented. The governing equations of the model correspond to a limiting case, for unimportant Coriolis acceleration, of those already investigated by Gutman and Malbakhov (1964).

The possible existence of two prototypical slope flow regimes (super- and subcritical), separated by a critical state, is highlighted. It proves useful to consider the analogy with the case of internal gravity waves, where forcing frequencies smaller or larger than N discriminate between propagating and evanescent waves, respectively (Nappo, 2013). Similarly, in our case, forcing at frequencies smaller (resp. greater) than N results in supercritical (resp. subcritical) slope flow.

Existing analytical models of slope flows, e.g. those by Prandtl (1942) and Defant (1949), are shown to correspond to special cases of the new, general solution. In particular, Defant's model coincides with a supercritical condition where the characteristic frequency of the surface forcing cycle is much smaller than the intrinsic frequency of buoyancy oscillations. Prandtl's model results from the same supercritical condition, when $\omega = 0$ and $\psi = \pi/2$. Differently from the Prandtl and Defant theories, the new model is well behaved for $N \rightarrow 0$ and $\alpha \rightarrow 0$, i.e. it naturally collapses to a subcritical regime, where turbulent diffusion is the sole process responsible for heat transfer in the atmosphere, in the absence of slope-parallel advection.

In general, the vertical variation of wind speed and temperature perturbations depends on the two length scales ℓ_+ and ℓ_- . When the difference between the two scales is large (see e.g. Figure 3), profiles of \bar{u} and $\bar{\theta}$ deviate considerably from those suggested by Prandtl theory. The most notable case in which this may happen

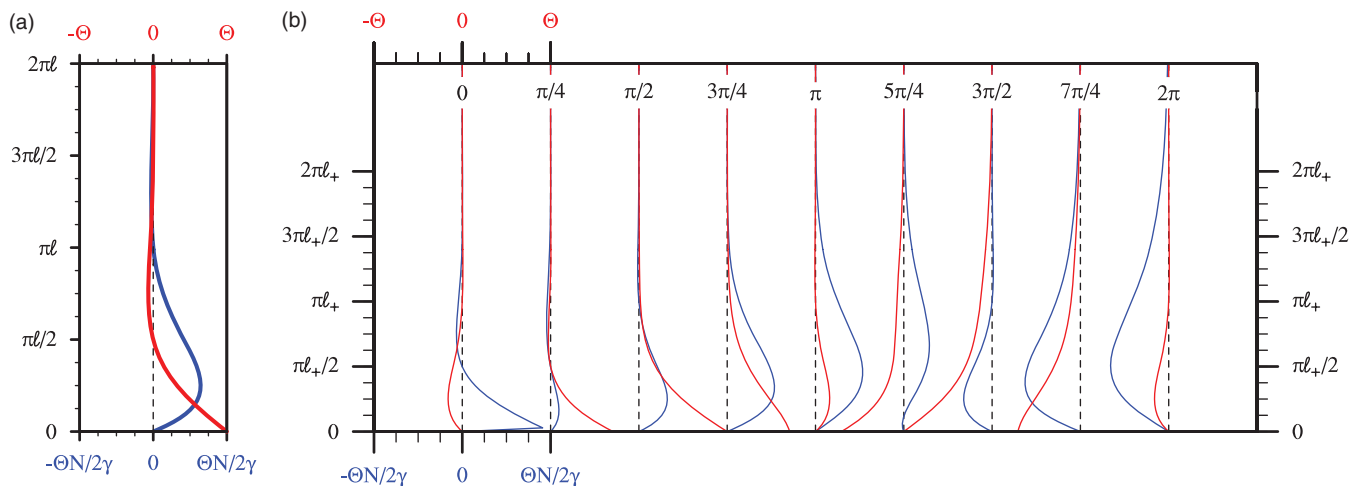


Figure 4. Same as in Figure 2, for a critical condition ($N_\alpha = \omega$). Numerical values: $\alpha = 0.41^\circ$, $\gamma = 0.003 \text{ K m}^{-1}$, $\psi = 0$.

is that of thermally forced flows developing in a nearly neutral atmosphere. Therefore, slope-normal profiles of temperature and wind speed should not be expected to match the Prandtl model, even approximately, in the late morning and afternoon stages of the diurnal cycle of mountain breezes, when anabatic flows occur in a context of weakening stratification due to the formation of a valley mixed layer (Serafin and Zardi, 2010a, 2011).

Time-dependent profiles of flow velocity and (potential) temperature similar to those derived in the present work were found by Shapiro and Fedorovich (2006) for flow along vertical plates immersed in a stably stratified environment. Interestingly, postulating the existence of harmonic solutions to the problem (as opposed to deriving their general form, as is done here) allows Shapiro and Fedorovich (2004a, 2006) to extend their model to the case $\text{Pr} \neq 1$. When $\text{Pr} = 1$, their solutions correspond essentially to a particular case of ours ($\alpha \rightarrow \pi/2$) and feature the same fundamental physical behaviour. In fact, the response of the system is found to depend on the relative magnitude of the forcing frequency with respect to the natural frequency of the environment, with resonant behaviour if the two are equal.

The present work, in analogy to Prandtl (1942) and Shapiro and Fedorovich (2004a, 2004b, 2006), stresses the importance of a particular aspect of stratified flows along heated or cooled surfaces. Namely, due to viscosity, upward (resp. downward) advection of warm (resp. cold) fluid generates a cold (resp. warm) anomaly with respect to the environment. In Prandtl's upslope flow model, for instance, reduced buoyancy for $\pi l/2 < n < 3\pi l/2$ limits upslope movement and causes the development of a weak compensation flow (an anti-slope current). This negative feedback process prevents velocity and temperature perturbations from extending to large distances from the surface and, in cases where the forcing remains constant in time, allows the flow to approach a steady state.

The key ingredients for this process to develop are stratification and parallel advection. No such flow pattern, and therefore no steady-state or steady periodic behaviour, can be established if either of the two is missing. For instance, thermal anomalies continuously spread out from a heated vertical plate if the environment is neutrally stratified (Shapiro and Fedorovich, 2004b). Similarly, thermal anomalies continuously diffuse away from a heated horizontal surface, given the absence of tilt promoting parallel advection, regardless of stratification (section 3.2 above).

As outlined in the Introduction and in section 2.1, the simple framework used by the Prandtl and Defant analytic slope wind models does not allow pressure–velocity correlations and therefore excludes internal gravity waves from the set of possible solutions. Consequently, even the present model cannot elucidate the possibly two-way interaction between gravity waves and slope flows, in particular during nocturnal hours. Indeed,

related phenomena, such as the possible impact of gravity waves on katabatic flow or the generation of internal gravity waves by katabatic winds, were documented and investigated by Poulos *et al.* (2000, 2007), Chemel *et al.* (2009) and Largeron *et al.* (2013).

Finally it is worth emphasizing that the present model can be extended rather easily, by means of series expansion or transform methods, in order to analyze the response of the atmosphere to impulsive or irregular temporal variations of temperature along a sloping surface. Also, effects related to the feedback exerted by slope flow systems on the background stability profile and more realistic spatially varying eddy diffusivities can be partially accounted for using perturbation methods (e.g. Grisogono *et al.*, 2014). However, substantial progress in understanding the properties of time-dependent thermally forced slope flows is expected to occur mostly by means of high-resolution numerical simulations, where turbulent exchange processes are resolved explicitly or parametrized adequately.

Acknowledgements

The Authors are grateful to two anonymous reviewers for their careful review and constructive comments. In particular, their mention of the valuable articles by Gutman and Malbakhov (1964) and Shapiro and Fedorovich (2006), which were previously unknown to the Authors, was highly appreciated. The Authors are also deeply grateful to Evgeny Borovin for his valuable help in translating from Russian the paper by Gutman and Malbakhov (1964).

References

- Axelsen S, van Dop H. 2009a. Large-eddy simulation of katabatic winds. Part 1: Comparison with observations. *Acta Geophys.* **57**: 803–836.
- Axelsen S, van Dop H. 2009b. Large-eddy simulation of katabatic winds. Part 2: Sensitivity study and comparison with analytical models. *Acta Geophys.* **57**: 837–856.
- Carslaw H, Jaeger J. 1959. *Conduction of Heat in Solids*. Oxford Science Publications, Clarendon Press: Oxford, UK.
- Chemel C, Staquet C, Largeron Y. 2009. Generation of internal gravity waves by a katabatic wind in an idealized alpine valley. *Meteorol. Atmos. Phys.* **103**: 187–194.
- Defant F. 1949. Zur Theorie der Hangwinde, nebst Bemerkungen zur Theorie der Berg- und Talwinde. *Arch. Meteorol. Geophys. Bioklimatol. A I*: 421–450.
- Ekman VW. 1905. On the influence of the Earth's rotation on ocean-currents. *Ark. Mat. Astron. Fys.* **2**: 1–53.
- Fedorovich E, Shapiro A. 2009. Structure of numerically simulated katabatic and anabatic flows along steep slopes. *Acta Geophys.* **57**: 981–1010.
- Grisogono B, Jurina T, Večenaj Ž, Güttler I. 2014. Weakly non-linear Prandtl model for simple slope flows. *Q. J. R. Meteorol. Soc.*, doi: 10.1002/qj.2406.
- Grisogono B, Oerlemans J. 2001. Katabatic flow: Analytic solution for gradually varying eddy diffusivities. *J. Atmos. Sci.* **58**: 3349–3354.
- Gutman LN, Malbakhov VM. 1964. On the theory of katabatic winds of Antarctic (in Russian). *Meteorol. Issled.* **9**: 150–155.

- Haiden T. 2003. On the pressure field in the slope wind layer. *J. Atmos. Sci.* **60**: 1632–1635.
- Khanna S, Brasseur JG. 1997. Analysis of Monin–Obukhov similarity from large-eddy simulation. *J. Fluid Mech.* **345**: 251–286.
- Largeroy Y, Staquet C, Chemel C. 2013. Characterization of oscillatory motions in the stable atmosphere of a deep valley. *Boundary-Layer Meteorol.* **148**: 439–454.
- Lumley J, Panofsky H. 1964. *The Structure of Atmospheric Turbulence. Interscience Monographs and Texts in Physics and Astronomy*. Interscience Publishers: New York, NY.
- Monin A, Yaglom A. 1971. *Statistical Fluid Mechanics: Mechanics of Turbulence*. MIT Press: Cambridge, MA.
- Nappo C. 2013. *An Introduction to Atmospheric Gravity Waves, International Geophysics Series*. Academic Press/Elsevier: San Diego, CA.
- Poulos GS, Bossert JE, McKee TB, Pielke RA. 2000. The interaction of katabatic flow and mountain waves. Part I: Observations and idealized simulations. *J. Atmos. Sci.* **57**: 1919–1936.
- Poulos GS, Bossert JE, McKee TB, Pielke RA. 2007. The interaction of katabatic flow and mountain waves. Part II: Case study analysis and conceptual model. *J. Atmos. Sci.* **64**: 1857–1879.
- Prandtl L. 1942. *Führer durch die Strömungslehre*, Chapter 5. Vieweg und Sohn: Braunschweig, Germany. [English translation: Prandtl L. 1952. Mountain and valley winds in stratified air, in *Essentials of Fluid Dynamics*: 422–425. Hafner Publishing Company: New York, NY].
- Schumann U. 1990. Large-eddy simulation of the upslope boundary layer. *Q. J. R. Meteorol. Soc.* **116**: 637–670.
- Serafin S, Zardi D. 2010a. Daytime heat transfer processes related to slope flows and turbulent convection in an idealized mountain valley. *J. Atmos. Sci.* **67**: 3739–3756.
- Serafin S, Zardi D. 2010b. Structure of the atmospheric boundary layer in the vicinity of a developing upslope flow system: A numerical model study. *J. Atmos. Sci.* **67**: 1171–1185.
- Serafin S, Zardi D. 2011. Daytime development of the boundary layer over a plain and in a valley under fair weather conditions: A comparison by means of idealized numerical simulations. *J. Atmos. Sci.* **68**: 2128–2141.
- Shapiro A, Fedorovich E. 2004a. Prandtl number dependence of unsteady natural convection along a vertical plate in a stably stratified fluid. *Int. J. Heat Mass Transfer* **47**: 4911–4927.
- Shapiro A, Fedorovich E. 2004b. Unsteady convectively driven flow along a vertical plate immersed in a stably stratified fluid. *J. Fluid Mech.* **498**: 333–352.
- Shapiro A, Fedorovich E. 2006. Natural convection in a stably stratified fluid along vertical plates and cylinders with temporally periodic surface temperature variations. *J. Fluid Mech.* **546**: 295–311.
- Shapiro A, Fedorovich E. 2010. Analytical description of a nocturnal low-level jet. *Q. J. R. Meteorol. Soc.* **136**: 1255–1262.
- Skyllingstad ED. 2003. Large-eddy simulation of katabatic flows. *Boundary-Layer Meteorol.* **106**: 217–243.
- Smith CM, Skillingstad ED. 2005. Numerical simulation of katabatic flow with changing slope angle. *Mon. Weather Rev.* **133**: 3065–3080.
- Sorbjan Z. 1989. *Structure of the Atmospheric Boundary Layer*. Prentice Hall: Englewood Cliffs, NJ.
- Stiperski I, Kavčić I, Grisogono B, Durran DR. 2007. Including Coriolis effects in the Prandtl model for katabatic flows. *Q. J. R. Meteorol. Soc.* **133**: 101–106.
- Veronis G. 1967. Analogous behavior of homogeneous, rotating fluids and stratified, non-rotating fluids. *Tellus* **19**: 326–336.
- Zammett RJ, Fowler AC. 2007. Katabatic winds on ice sheets: A refinement of the Prandtl model. *J. Atmos. Sci.* **64**: 2707–2716.
- Zardi D, Whiteman CD. 2013. Diurnal mountain wind systems. In *Mountain Weather Research and Forecasting. Recent Progress and Current Challenges*, Springer Atmospheric Sciences, Chow FK, De Wekker SFJ, Snyder B. (eds.): 37–122. Springer: Berlin.